ACS APPLIED MATERIALS & INTERFACES

Research Article

www.acsami.org

Probing the Adjustments of Macromolecules during Their Surface Adsorption

Pengxiang Jia,[†] Min He,[†] Yongkuan Gong,*[,†] Xiao Chu,[‡,†] Jingfa Yang,*[,‡] and Jiang Zhao[‡]

[†]Key Laboratory of Synthetic and Natural Functional Molecule Chemistry of Ministry of Education, College of Chemistry and Materials Science, Northwest University, Xi'an, Shaanxi 710069, China

[‡]Beijing National Laboratory for Molecular Science, Institute of Chemistry, Chinese Academy of Sciences, Beijing 100190, China

ABSTRACT: Thiol-terminated polymers poly(2-methacryloyloxyethyl phosphorylcholine) (PMPC-SH), poly(*N*,*N*-isopropylacrylamide) (PNIPAM-SH), and poly(*tert*-butyl acrylate) (PtBA-SH) were synthesized, and the polymers were grafted on the gold surfaces of quartz crystal microbalance with dissipation (QCM-D) and surface plasmon resonance (SPR) sensor chips to form brushes. The grafting process of the polymer brushes as well as protein adsorption onto the brush layers was monitored by *in situ* QCM-D and SPR techniques. By examining the changes in frequency and dissipation factor as well as the value of $\partial D/\partial f$ from QCM-D measurements, different stages of the polymer grafting and protein adsorption are distinguished. The most interesting discovery is the conformation change of BSA protein adsorption from a weakly adsorbed native state to a strongly immobilized denatured state on the polymer brushes. The corresponding change in BSA adsorption from a reversible state to an irreversible state was confirmed by SPR measurements. The adsorption of protein on the polymer brushes' surface relies largely on interaction between the protein and the polymers, and the stronger hydrophilicity of the surfaces is proved to be more effective to suppress the protein adsorption. Analysis of the *D*−*f* plot of QCM-D measurements helps to characterize different binding strength of protein and the underlying polymer surface.

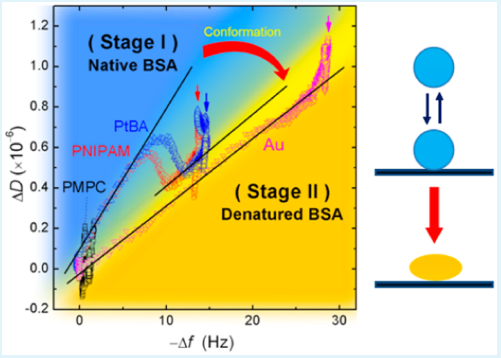

KEYWORDS: *protein adsorption, QCM-D, SPR, conformation, polymer brushes*

INTRODUCTION

Although being a highly debated topic, surface adsorption of proteins has been attracting intensive research attention for decades.[1] It is not only an important aspect regarding the functionality of biosubstances at interfaces but also related to a few essential issues of industry and biomedical applications, such as antifouling of marine vehicles and implantation of artificial devices in human bodies and so forth. It has been shown that a number of factors influence protein adsorption on surfaces, including the chemical structure of the surfaces, hydrophobicity, ionic or electrostatic interaction, surface morphology, and so forth.[2−6] Attention has been paid to the competing effect of the above factors influencing the adsorption. For example, hydrophilic modification of the surface by polymers such as PEG[7,8] or zwitterionic polymers[9−14] can reduce protein adsorption. On the other hand, there have been recent studies showing that highly hydrophobic films coated with perfluorinated side-chain polymers were more efficient in decreasing the fouling of *Pseudomonas putida* than hydrophilic surfaces coated with PEG.[15,16] These phenomena indicate that the investigation into the principle of protein adsorption on various surfaces is very important despite the existence of controversies. Apart from a number of aspects regarding protein adsorption, such as amount of adsorption, adhesion energy, adsorption kinetics, and so forth, the adjustment or change of conformation of proteins as well as that of the underlining surface should also be an important issue. This piece of information is important as it can expose the real time picture of protein adsorption and can really help to understand the physical mechanism and to manipulate for optimal performance.

From the experimental point of view, various methods have been used to study surface adsorption of proteins.[17] Regarding the real-time kinetics of adsorption, both microscopic and spectroscopic techniques have been applied, such as the attenuated total reflection-Fourier transform infrared spectroscopy (ATR-FTIR),[18−22] grazing angle Fourier transform infrared spectroscopy (GA-FTIR),[23] surface plasmon resonance (SPR),[24,25] and atomic force microscopy (AFM).[26] Although rich information has been provided using these techniques, such as information about the amount of the adsorption, less information has been available on the conformation changes of the adsorbate as well as the underlying surfaces.

Surface sensitive techniques are believed to be helpful to bring new insight into this problem. Quartz crystal microbalance with dissipation (QCM-D) is a very sensitive technique which allows simultaneous measurements of mass and viscoelasticity change of a surface by measuring the changes

Received: August 23, 2014
Accepted: March 11, 2015
Published: March 11, 2015

DOI: 10.1021/acsami.5b01138
ACS Appl. Mater. Interfaces 2015, 7, 6422−6429

Scheme 1. Synthesis of Thiol Terminated Polymers and Structures of Monomers, 2-Methacryloyloxyethyl Phosphorylcholine (MPC), *N*-Isopropylacrylamide (NIPAM), and *tert*-Butyl Acrylate (tBA)

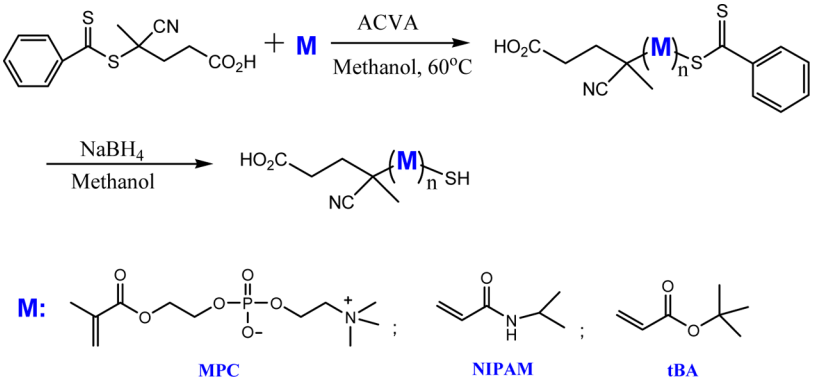

of resonant frequency (f) and energy dissipation (D) in a noninvasive manner.[27] The QCM-D can measure the mass change on the surface of the quartz chip on the order of 1.0×10^{-9} g cm^{-2}, even for the measurements in the liquid phase. This capability can, apparently, allow measurements of the dynamic behavior of protein adsorption.[28−30] QCM-D has also been proved useful for studying conformational changes of macromolecules. For example, it has been applied to study the collapse and swelling or mushroom-to-brush transition of polymer brushes.[31−33] Regarding changes happening with adsorbed proteins, QCM-D has been proved to be effective. For example, there have been studies on the structural changes of hemoglobin during adsorption to hydrophobic self-assembled methyl-terminated thiol monolayer on gold surfaces.[30] The results suggested that, below the isoelectric points of hemoglobin, there are two states of the adsorbed proteins, a layer bound more rigidly to the solid surface, presumably consisted of denatured proteins and another layer bound more loosely, presumably made of native-like proteins. The time-resolved feature of QCM-D measurements even allows measurements of kinetics of protein conformation change at interfaces. However, the information about conformation changes received from QCM-D is rather indirect.

Surface plasmon resonance (SPR) is another sensitive method for surface adsorption analysis. This method relies on the coupling of the incident radiation into the surface plasma, which depends on the refractive index of the surface layer. Because of the strict condition of surface plasmon coupling, SPR has been proved to be very sensitive plus its additional advantage of being label-free and noninvasive leading to its effectiveness in the study of protein adsorption.[34] For example, the resonance angle of SPR varies depending on the refractive index of the protein layer on the surface, and by measuring the shift of the coupling angle one can determine the "dry" mass of the adsorbed protein.[35]

Probing the surface with the combination of QCM and SPR can help us understand the process in a more comprehensive way. QCM is a mechanical probing method detecting the variation in the electromechanical response of a shear oscillating piezoelectric sensor caused by total changes of mass and viscoelasticity due to the adsorption of biomolecules, with solvent molecules coupled to the system,[36,37] while SPR sensitively detects the changes in refractive index of the layer caused by adsorption.[35] It is envisioned that these sensitive methods may be able to detect tiny changes happening during the process of adsorption which may not be sensible by other techniques, for example, the change of conformation of proteins as well as synthetic polymers.

Motivated by the possible advantage of the combination of QCM-D and SPR, the adsorption of a model protein, bovine serum albumin (BSA), onto polymer brushes is investigated. Three kinds of thiol terminated polymers with different hydrophilicity and hydrophobicity were synthesized, such as PMPC, PNIPAM, and PtBA, and their grafting process as well as the adsorption of BSA onto the grafted surfaces was monitored by QCM-D. The SPR technique was also employed to determine the real-time adsorption and desorption of BSA on the grafted polymer brush surfaces. The results provide interesting information on the kinetics of the grafting process and more importantly the surface dependent adjustment of the adsorbed protein structure. This kind of protein adsorption understanding may promote the development of more efficient antibiofouling polymer brushes and application in various biomedical applications.

EXPERIMENTAL SECTION

Materials. 2-Methacryloyloxyethyl phosphorylcholine (MPC) was purchased from Biocompatibles International PLC (U.K.). *N*-Isopropylacrylamide (NIPAM), *tert*-butyl acrylate (tBA), and 4,4′-azobis(4-cyanovaleric acid) (ACVA) were purchased from Aladdin (Beijing, China). 4-Cyano-4-(phenylcarbono-thioylthio) pentanoic acid (CTP), and bovine serum albumin (BSA) were purchased from Sigma-Aldrich. All materials mentioned above were used without further purification. The water used was purified by filtration through Millipore Gradient system after distillation, giving a resistivity of 18.2 MΩ cm.

Synthesis of Thiol-Terminated PMPC, PNIPAM, and PtBA. Dithioester terminated MPC polymer (PMPC), NIPAM polymer (PNIPAM,) and tBA polymer (PtBA) were synthesized by reversible addition−fragmentation chain transfer (RAFT) polymerization in methanol at 60 °C, using ACVA as the initiator and CTP as the chain transfer agent. The synthesis of the polymers and the monomer structures are shown in Scheme 1. In a typical protocol, MPC (2.0 g, 6.8 mmol), CTP (0.030 g, 0.10 mmol), and ACVA (1.5×10^{-2} g, 0.052 mmol) were dissolved in 6 mL of methanol in a 10 mL Schlenk tube. The solution was then degassed via three freeze−vacuum−thaw cycles and placed in a 60 °C oil bath for 11 h. The polymer was obtained by precipitation in a large quantity of acetone (for PMPC), diethyl ether (for PNIPAM), or 1:1 methanol/water (for PtBA). Dithioester terminated polymer methanol solutions (20 mL, 1.5 mg mL^{-1}) were mixed with 2.0 mL of $NaBH_4$ methanol solution (1.0 M). The mixture was stirred at room temperature for 5 days so that the end groups of the polymer chains were completely reduced into thiols.[38] The molecular weight and polydispersity were measured by

DOI: 10.1021/acsami.5b01138
ACS Appl. Mater. Interfaces 2015, 7, 6422−6429

gel permeation chromatography (GPC) with aqueous eluent (for PMPC) or tetrahydrofuran eluent (for PNIPAM and PtBA).

Fabrication of Polymer Brushes with Thiol-Terminated Polymers. Polymer brushes were grafted onto the gold surface of the QCM-D and SPR sensor chips. The chips were cleaned carefully with acetone and pure water before being treated in an UV/ozone chamber for 30 min, followed by 30 min of oxygen plasma treatment. The grafting of polymer chains onto the gold-coated QCM-D and SPR chips was performed by immersing the chips in methanol solution of the thiol-terminated polymers with a concentration of 1.5 mg mL^{-1} for 12 h. After this grafting reaction, a monolayer of the polymer brushes formed on the substrates and the physically adsorbed polymers were washed off by intensive rinsing with ethanol.

For *in situ* characterization of the grafting process by QCM-D, the cleaned gold-covered quartz chip was first mounted into the liquid cell of the instrument. Afterward, the polymer solution was directly introduced by a microprocessor-controlled tubing pump (ISMATEC, IDEX, America) with a constant flow rate of 150 μL min^{-1}.

Thickness Characterization by Ellipsometry. The film thickness of the grafted polymer layer on gold surfaces was measured by an ellipsometer (M-2000 V, J. A. Woollam Co., Lincoln, NE) at a fixed incident angle of 70°. Five separate measurements were conducted at different locations on each sample.

X-ray Photoelectron Spectroscopy. The elemental composition of the grafted surfaces was determined by X-ray photoelectron spectroscopy (XPS). The spectra were measured by an ESCALab220i-XL system (VG Scientific, U.K.) using Mg Kα radiation (300 W, 1253.6 eV) with the air pressure of 3×10^{-9} mbar. All spectra were collected at an electron takeoff angle of 70° from the surface. Binding energies were calibrated relative to the C 1s peak (284.8 eV) from hydrocarbons adsorbed on the surface of the samples.

Quartz Crystal Microbalance with Dissipation (QCM-D) Measurements. QCM-D measurements were conducted with a Q-sense E1 microbalance (Biolin Scientific, Sweden). The principle and applications of QCM-D have been reviewed previously.[27] A tracer amount of adsorbate onto the chip induces a decrease in resonant frequency (Δf), which is proportional to the mass change (Δm) of the adsorbate. For QCM-D operating in vacuum or air, the well-known Sauerbrey equation is applied for a rigidly adsorbed layer evenly distributed:[39] $\Delta m = -(\rho_q l_q/F_0)(\Delta f/n) = -C(\Delta f/n)$, where f_0 is the fundamental frequency, ρ_q and l_q are the specific density and thickness of the quartz crystal, respectively. Another important parameter, the dissipation factor (D), is defined as $D = (E_d/2\pi E_s)$,[40] where E_d is the energy dissipated during one oscillation and E_s is the energy stored in the oscillating system. The measurement of ΔD is based on the fact that the voltage over the crystal decays exponentially as a damped sinusoidal when the driving power of a piezoelectric oscillator is switched off.[40] In the present study, all the results obtained were from the measurements of frequency and dissipation changes at the third overtone (n = 3). All the experiments were performed in aqueous solution at 23 °C, and the flow rate was 150 μL min^{-1}.

Surface Plasmon Resonance (SPR) Measurements. SPR measurements were carried out with a Reichert SR7500DC system (Reichert Technologies Life Sciences) at 25 °C. Prior to the measurement of protein adsorption, a signal baseline was established by flowing PBS buffer or PBS-SDS(PBS buffer containing 1% sodium dodecyl sulfate) at a rate of 50 μL min^{-1} through the sensor for about 10 min. For protein adsorption experiments, BSA dissolved in the PBS buffer with a concentration of 1.0 mg mL^{-1} was applied by flow through the sensor channels for 1.0 or 20.0 min, followed by a rinse with PBS buffer or PBS-SDS solution to remove the unbound or loosely adsorbed protein molecules. Protein adsorption was quantified by measuring the change in response units (RU) from the buffer baselines before and after protein adsorption. The RU change was converted to the amount of adsorbed protein. For the SPR sensor used in this work, 1 RU corresponds to a surface coverage of about 0.1 ng cm^{-2} adsorbed protein.[41,42]

RESULTS AND DISCUSSION

Characterization of Polymer Coated Surfaces. The polymer structures of PMPC, PNIPAM, and PtBA synthesized by RAFT polymerization are drawn in Scheme 1 and their parameters are shown in Table 1. Compared with the other two polymer samples, PMPC has a much lower polydispersity. This is attributed to the compatibility of the chain transfer reagent, CTP, in the RAFT polymerizations of MPC.[43,44] The parameters of the grafted polymer films are also listed in Table 1, in which the dry thicknesses of PMPC, PNIPAM, and PtBA layers measured by ellipsometry are 1.74, 0.63, and 1.82 nm, respectively. The graft density (σ) was calculated using the dry thickness of each polymer layer from the equation $\sigma = N_A h\rho/M_n$,[45] where N_A is the Avogadro's constant, h the layer thickness determined by ellipsometry, ρ the density of each dry polymer layer, and M_n the number-average molecular weight of the polymers. The grafting densities of PMPC, PNIPAM, and PtBA layers were calculated to be 0.13, 0.22, and 0.20 chains nm^{-2}, respectively, corresponding to an average interchain distance of 2.8, 2.1, and 2.2 nm, respectively. Obviously, the interchain distance is comparable to the value of root-mean-square end-to-end distance calculated by freely rotating chain model of the grafted polymer (1.8, 1.6, and 2.1 nm for PMPC, PNIPAM, and PtBA, respectively), indicating the formation of loosely packed polymer brushes on the gold surfaces. The grafting densities are comparable to the values of brushes fabricated by "graft from" method.[46] Such high values of grafting density are attributed to two origins: (1) the strong interaction between thiol group of the polymer chain and gold surface, (2) the relatively short polymer chains, the degree of polymerization of all three polymers, i.e., PMPC, PNIPAM, and PtBA, are 36, 27, and 46, respectively.

Table 1. Parameters of the Polymer Samples and the Grafted Brushes

sample	M_n (g mol^{-1})	M_w/M_n	thickness (nm)	ρ (g cm^{-3})	graft density (chains nm^{-2})
PMPC	10472	1.09	1.74	1.28[47]	0.13
PNIPAM	3071	1.54	0.63	1.76[48]	0.22
PtBA	5861	1.75	1.82	1.05[49]	0.20

Characterization of chemical composition of the polymer layer by XPS spectroscopy further proved the presence of designed polymer brushes despite their small thickness. As shown in Table 2, the surface element compositions of PMPC, PNIPAM, and PtBA layers are calculated from the XPS peak areas of the elements and their relative sensitivity. The significant contents of the C, N, O, S, and P elements appeared on the gold surfaces confirm the PMPC, PNIPAM, and PtBA polymer layers. On the other hand, the relatively high concentration of the substrate gold signal supports the small

Table 2. Elemental Composition of the Polymer Brush Surfaces Measured by XPS

	relative molar ratio of surface element (mol %)					
samples	C 1s	N 1s	O 1s	S 2p	P 2p	Au 4f
PMPC	39.26	1.54	22.76	1.60	2.75	32.09
PNIPAM	39.90	3.38	11.51	2.90	0.00	42.30
PtBA	48.73	0.00	14.68	2.11	0.00	34.48

DOI: 10.1021/acsami.5b01138
ACS Appl. Mater. Interfaces 2015, 7, 6422−6429

film thickness of the polymers, which is smaller than the maximum detection depth (~9 nm) of XPS.[13]

***In Situ* Characterization of the Polymer Grafting Process by QCM-D.** The grafting process of the dithioester terminated PMPC (PMPC-DTE) and thiol-terminated PMPC (PMPC-SH) chains onto the gold surface of QCM-D chips were monitored by using *in situ* QCM-D measurements, as displayed in Figure 1. The process is clearly demonstrated by

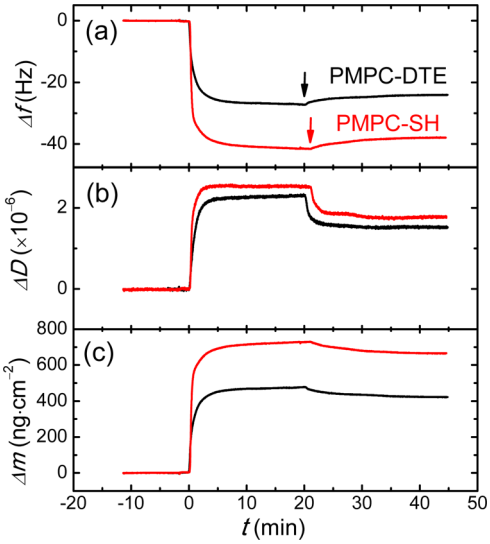

Figure 1. Time profile of the frequency shift (Δf) (a), dissipation shift (ΔD) (b), and Sauerbrey mass change (c) of PMPC-DTE and PMPC-SH with a concentration of 1.5 mg mL^{-1} during the grafting process. The moment of $t = 0$ denotes the point where the solution for grafting is introduced. The arrows denote the moment of exchanging the polymer solution with pure water.

the temporal profile of the frequency change and dissipation change (Figure 1a,b). Upon addition of the polymer solution (at $t = 0$), a rapid frequency decrease corresponding to the mass increase was observed, followed by a saturation. The value of D increases with a similar time profile. The increase of D indicates more energy dissipated into the solution as more polymers are adsorbed. The effect of rinsing (denoted by the arrows in Figure 1a) is also clearly demonstrated showing the wash-off of the physically adsorbed polymers. The difference in Δf by rinsing is rather small, showing the profoundness and the stability of the chemical adsorption.

The current experimental condition satisfies the requirement for the application of the well-known Sauerbrey equation,[27] i.e., $-\Delta D_n/(\Delta f_n/n) \leq 4 \times 10^{-7}$ Hz^{-1} (the current maximum value of $-\Delta D_n/(\Delta f_n/n)$ is 3.9×10^{-7} Hz^{-1}). Therefore, the mass change (Figure 1c) can be deduced directly from the frequency data. The values of the mass of PMPC-SH measured by QCM-D after rinsing (~660 ng cm^{-2}) is obviously higher than that calculated from the value of grafting density (~220 ng cm^{-2}), and the difference is attributed to the large amount of solvent incorporated in the QCM-D measurements.[36,37] The mass change brought by PMPC-DTE is always smaller than that by PMPC-SH, indicating a much stronger interaction between the thiol end group of PMPC-SH polymer and the gold surface than that of the dithioester end group polymer with the gold surface.

The plot of ΔD against Δf (termed as D–f plots) is used to study the grafting process, as it has been proved informative on the conformational changes of macromolecules at surfaces.[30−33,50,51] Figure 2 displays the D–f plot of the grafting

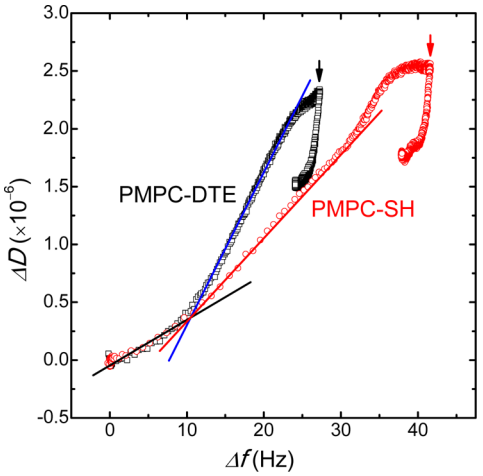

Figure 2. Plot of ΔD against Δf of PMPC-DTE and PMPC-SH during their grafting process onto gold surfaces. The arrows denote the moment of exchanging the polymer solution with pure water.

process of PMPC-DTE and PMPC-SH. Apparently, the data exhibit two stages with two different values of the slope ($\partial D/\partial f$). In the first stage, PMPC-DTE and PMPC-SH have an identical $\partial D/\partial f$ value, demonstrating their similar conformation at the surface. This is understood as the process of the polymer chains occupying the empty surface, during which the chains take a pancake-like conformation. In the second stage, two data sets diverge, both exhibiting larger slope than that of the first stage. The smaller slope of the first stage was associated with a more rigidly attached polymer taking on a pancake conformation, whereas a more fluffy conformation of the loosely packed brushes with the increase amount of the grafting polymer chains in the second stage. Therefore, the data demonstrate a pancake-to-brush transition during the grafting process.[33] It is also noted that, in the second stage, the $\partial D/\partial f$ values of PMPC-SH is smaller than that of PMPC-DTE, showing that the grafting process of PMPC-SH forms a denser and more rigid layer than that by PMPC-DTE. It is reported that both dithioester and thiol end-capped polymers can bind directly on the gold surface.[52,53] Since the dithioester group is much larger than the thiol group, the grafted mass and density of PMPC-DTE is smaller than that of PMPC-SH (Figure 1). Accordingly, the grafting process of PMPC-SH forms a denser and more rigid layer than that by PMPC-DTE. As high surface density of a grafted polymer brush usually shows excellent biocompatibility, this investigation is focused on the thiol immobilized polymer brushes.

***In Situ* Characterization of BSA Adsorption Kinetics by QCM-D.** The adsorption kinetics of BSA onto bare gold, PNIPAM, PtBA, and PMPC grafted polymer brushes is investigated *in situ* by QCM-D. As shown in Figure 3, the results clearly demonstrate the drastic suppression of protein adsorption by PMPC brushes. The adsorbed mass on PMPC surface is only 18.7 ng cm^{-2}, an order of magnitude lower than that on PtBA and PNIPAM (~240.0 ng cm^{-2}). As a reference, the data on the bare gold surface is also shown (496.8 ng cm^{-2}). Therefore, the suppression of protein adsorption by polymer brushes is obvious, the surface modification with PNIPAM and PtBA brings about 52% reduction of BSA

DOI: 10.1021/acsami.5b01138
ACS Appl. Mater. Interfaces 2015, 7, 6422−6429

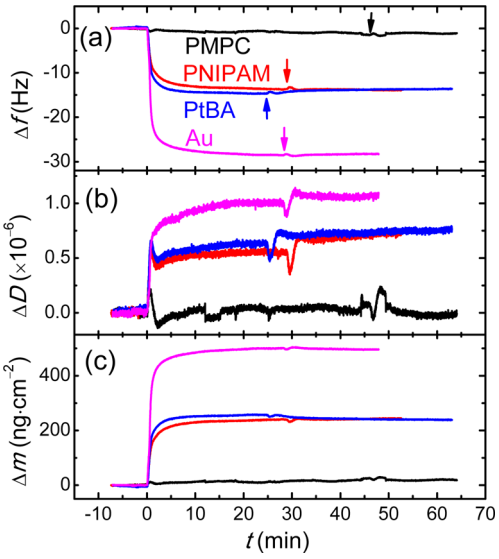

Figure 3. Time profile of the frequency shift (Δf) (a), dissipation shift (ΔD) (b), and Sauerbrey mass change (c) of surfaces coated with PMPC, PNIPAM, and PtBA during the adsorption of BSA with a concentration of 1.0 mg mL^{-1}(in 10 mM PBS buffer, pH 7.4).The moment of t = 0 denotes the point where the BSA solution is introduced. The arrows denote the moment when PBS buffer solution was introduced for rinsing.

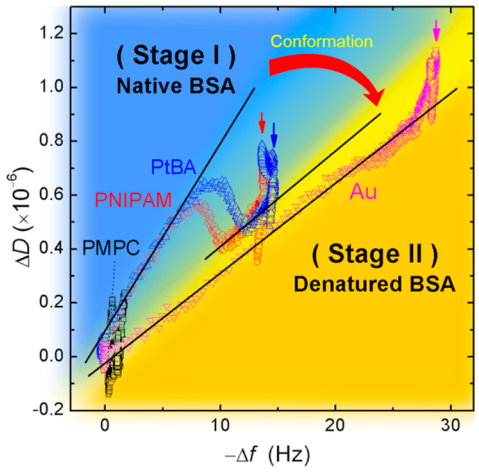

Figure 4. Plot of ΔD against Δf of a few surfaces during the adsorption of BSA. The moment of exchanging the BSA solution with PBS buffer solution was marked by arrows.

adsorption and 96% reduction of BSA adsorption by PMPC coating.

The changes in the dissipation (Figure 3b) differ largely from those in frequency. Not like the monotonous changes of Δf, the ΔD values of BSA adsorption on PMPC, PNIPAM, and PtBA brushes show a sharp decrease around 1.0 min of the adsorption and then increase again slowly around 2.0 min. As a comparison, the ΔD values of BSA adsorption on the bare gold surface do not show such a change. The variation of the ΔD value with polymer coated surfaces is due to the adjustment process between the adsorbed BSA protein and the underlining polymer brushes during the adsorption, a process consisting of a few steps: the binding between the protein and the polymer brushes and the conformation adjustment of the protein and the polymer brushes to maximize their contact and minimize their free energy.

The D–f plots of the adsorption process of BSA provide more information on the binding of the protein on the polymer grafted surfaces (Figure 4). The adsorption of BSA onto PNIPAM and PtBA surfaces exhibits two stages. In stage I with Δf less than 7 Hz, both $\partial D/\partial f$ data of PNIPAM and PtBA systems show almost an identical value, demonstrating the similar conformation of BSA protein and its interaction with the brush surfaces. What is really interesting is the transition from a higher $\partial D/\partial f$ value to a lower one as the adsorption process proceeds. As shown in Figure 4, the $\partial D/\partial f$ value of PNIPAM and PtBA systems changes from 8.3×10^{-8} Hz^{-1} (in stage I) to 3.3×10^{-8} Hz^{-1}(in stage II) after Δf exceeds 10 Hz. Interestingly, the $\partial D/\partial f$ value in stage II is quite similar to that on bare gold surface and remains constant before rinsing by PBS.

The comparison between the behaviors of BSA on the bare gold surface and the polymer brush surfaces renders interesting findings. The $\partial D/\partial f$ value of BSA on the bare gold does not change while vast changes occur with BSA on PNIPAM and PtBA brushes, which evidence the adjustments of the protein and the polymer chains upon the adsorption of the proteins. It is attributed to the process of the protein maximizing its contact with the polymer brush surfaces. It is envisioned that the BSA protein particle of ellipsoidal shape first contacts with the surface (stage I) and then adjusts its conformation or orientation to maximize its interaction with the polymer brushes (stage II). The ellipsoidal BSA protein (dimensions, 140 Å × 40 Å × 40 Å[54]) should adsorb on the surface rapidly with its axis orienting along the normal direction of the surface due to a high mobility along its axis. The rapid adsorption (stage I) is supported by the steep changes in frequency, dissipation, and mass of the BSA adsorption within 1 min as shown in Figure 3. More importantly, the dramatic changes in dissipation from rapid increase to steep decrease appear during the BSA adsorption on all three polymer brushes. The rapid decrease in dissipation with increasing adsorption amount suggests clearly a conformation change and the adsorption transforms to stage II. Thus, a more rigid structure of BSA adsorption is formed by either lying parallel to the surface or inserting into the PNIPAM or PtBA brushes via the attraction from the surface. Because the average distance between the grafted chains is relative big (approximately 2.0 nm), the hindrance for penetration is rather small. On the other hand, the self-adjustments of protein itself can also be possible. The protein takes a native-like state at the early stage (I) of the adsorption and then adjusts its conformation in the second stage (II). The conformational adjustment results in a stronger binding to the surface, presumably being in a denatured state.[23,30] For BSA adsorbed on bare gold surface, only one $\partial D/\partial f$ value was observed, which is similar, surprisingly, to that of BSA adsorption on PNIPAM and PtBA surfaces in the second stage (II). The data show the effect of the strong attraction between the gold surface and BSA molecules, which results in an immediate adjustment of the protein's conformation together with the tight surface binding. One more note: although the PMPC surface shows the least amount of BSA adsorption, the value of ΔD (<0.25×10^{-6}) and $-\Delta f$ (<2.0 Hz) are too small to have a reliable $\partial D/\partial f$ analysis.

***In Situ* Characterization of BSA Adsorption Kinetics by SPR.** The adsorption kinetics of BSA from PBS buffer solution onto the different surfaces was investigated *in situ* by SPR measurements and the adsorption amount is shown in Table 3.

DOI: 10.1021/acsami.5b01138
ACS Appl. Mater. Interfaces 2015, 7, 6422−6429

Table 3. Adsorption Amount of BSA with a Concentration of 1.0 mg mL^{-1} (in 10 mM PBS Buffer, pH 7.4) onto Different Polymer Brushes Measured by SPR and QCM-D[a]

samples	adsorption amount (ng cm^{-2})		
	SPR (1 min)	SPR (20 min)	QCM-D
PMPC	5.6	13.5	18.7
PNIPAM	36.9	41.2	240.7
PtBA	54.9	53.7	244.7
Au	75.3	127.2	496.8

[a]PBS buffer was used to establish the signal baseline and remove the unbound protein molecules.

The results show a very fast adsorption of BSA, the adsorption amounts of 1.0 and 20.0 min adsorptions are almost at an identical level for PNIPAM and PtBA surfaces, while the adsorption amount on the PMPC surface is much lower. It is noted that the adsorbed amount measured by SPR is on the same order of that measured by QCM-D, though the values measured by SPR are always lower than those by QCM-D due to two possible reasons: (1) SPR only determines the "dry" mass of the adsorbed protein,[35] while QCM-D measures the adsorption of protein as well as the water coupled on it;[36,37] (2) the flow rate and adsorption time of SPR experiment is lower than that of QCM-D.

The adjustment of proteins and the underlying polymer layers is again clearly evidenced by SPR measurements on the effect of different adsorption time, with PBS-SDS solution (PBS buffer containing 1% sodium dodecyl sulfate) serving as the rinsing fluid to remove the loosely bound protein molecules. For the bare gold surface, no desorption of BSA is observed upon rinsing with PBS-SDS solution. On the contrary, for polymer surfaces, the adsorbed BSA is almost totally removed when the adsorption time is 1.0 min, though no more removal is observed for adsorption of 20.0 min (Figure 5). This phenomenon is observed for all three different polymer surfaces studied, with the final adsorption amounts differing on polymer type, the adsorption amounts have the order from high to low on the PtBA, PNIPAM, and PMPC surfaces.

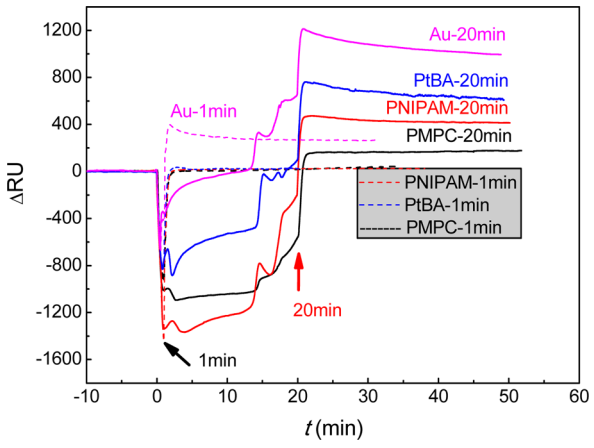

Figure 5. Adsorption profiles of BSA with a concentration of 1.0 mg mL^{-1}(in 10 mM PBS buffer, pH 7.4) onto different polymer layers by SPR measurements. PBS-SDS (PBS buffer containing 1% sodium dodecyl sulfate) solution was used to establish the signal baseline and remove the unbound protein molecules. The moment of $t = 0$ denotes the point where the BSA solution is introduced. The arrows denote the moments of PBS-SDS elution after the BSA adsorption for 1 and 20 min.

The results demonstrate the predominant effect of interaction between proteins and the polymers, based on two experimental facts. First, the amount of adsorption does NOT have noticeable correlation with the grafting density and therefore the major contribution of proteins' penetration into the brushes can be excluded. This is further proved by the highest adsorption amount on the nonpermeable PtBA layer, which is not swelled in aqueous medium. Second, a good correlation is discovered with hydrophobicity of the underneath polymer layer, the least adsorption happens on the most hydrophilic PMPC brushes while the most adsorption happens with the most hydrophobic PtBA brush layer.

Therefore, the results got from SPR and QCM-D support each other. It is obvious that the BSA proteins bind loosely to the polymer surface at the early stage of adsorption and they adjust their conformation in the later stage, establishing stronger binding to the surface.

By comparing the results by QCM-D and SPR, it is discovered that, for the present system, a reversible adsorption of BSA is found when the $\partial D/\partial f$ value is higher than 8.3×10^{-8} Hz^{-1} and irreversible adsorption is found when $\partial D/\partial f$ value is lower than 3.3×10^{-8} Hz^{-1}. This can be a new method to judge the status of adsorption and may be applied to other systems.

As the key problem of proteins adsorption, investigation of the conformation adjustment or change of proteins is challenging due to the complexity of the interplay between external factors, protein and surface properties. We have noticed that there have been continuous efforts in this direction. For example, people have spectroscopy and microscopy to study the structure and its evolution of adsorbed proteins.[18−26,30] However, it has been a challenge to study the structural evolution of the protein during its adsorption process by an *in situ* manner. The current study takes the advantage of the high sensitivity as well as the good time resolution of QCM-D and SPR, providing the clear evidence of the conformation adjustment process of BSA protein adsorption on polymer coatings. As far as we know, there has not been a study providing such information.

CONCLUSION

The adsorption of BSA protein and synthetic polymers onto the solid−liquid interfaces of QCM sensors can be detected sensitively by monitoring the changes in the resonance frequency and dissipation factor. By examining the value of $\partial D/\partial f$, different stages of BSA adsorption have been distinguished in which the adsorbed proteins adjust their conformation, presumably from the native state to the denatured state. The process of adjustments of proteins and the polymers upon surface adsorption is further verified by SPR experiment. The interaction of BSA molecules strengthened after prolonged adsorption. The adsorption of protein on polymer brushes' surface relies largely on interaction between the protein and the polymer, and hydrophilicity is proved to be effective to suppress the protein adsorption. Analysis of the $D-f$ plot of QCM-D measurements helps to characterize the different binding strengths of the protein and the underlying polymer surface.

AUTHOR INFORMATION

Corresponding Authors

*E-mail: gongyk@nwu.edu.cn.

DOI: 10.1021/acsami.5b01138
ACS Appl. Mater. Interfaces 2015, 7, 6422−6429

*E-mail: yangjf@iccas.ac.cn.

Notes

The authors declare no competing financial interest.

■ ACKNOWLEDGMENTS

This work is partially supported by the National Natural Science Foundation of China (Grants 21304075 and 51173197), Specialized Research Fund for the Doctoral Program of Higher Education (Grant 20126101120009), China Postdoctoral Science Foundation, Natural Science Basic Research Plan in Shaanxi Province of China Program (Grant 2012JQ2008), and Scientific Research Program Funded by Shaanxi Provincial Education Department (Grant 12JK0604).

■ REFERENCES

(1) Rabe, M.; Verdes, D.; Seeger, S. Understanding Protein Adsorption Phenomena at Solid Surfaces. *Adv. Colloid Interface Sci.* **2011**, *162*, 87−106.
(2) Czeslik, C. Factors Ruling Protein Adsorption. *Z. Phys. Chem.* **2004**, *218*, 771−801.
(3) Mrksich, M.; Whitesides, G. M. Using Self-Assembled Monolayers to Understand the Interactions of Man-Made Surfaces with Proteins and Cells. *Annu. Rev. Biophys. Biomol. Struct.* **1996**, *25*, 55−78.
(4) Cox, J. D.; Curry, M. S.; Skirboll, S. K.; Gourley, P. L.; Sasaki, D. Y. Surface Passivation of a Microfluidic Device to Glial Cell Adhesion: a Comparison of Hydrophobic and Hydrophilic SAM Coatings. *Biomaterials* **2002**, *23*, 929−935.
(5) Genzer, J.; Arifuzzaman, S.; Bhat, R. R.; Efimenko, K.; Ren, C.; Szleifer, I. Time Dependence of Lysozyme Adsorption on End-Grafted Polymer Layers of Variable Grafting Density and Length. *Langmuir* **2012**, *28*, 2122−2130.
(6) Fang, F.; Szleifer, I. Effect of Molecular Structure on the Adsorption of Protein on Surfaces with Grafted Polymers. *Langmuir* **2002**, *18*, 5497−5510.
(7) Schilp, S.; Kueller, A.; Rosenhahn, A.; Grunze, M.; Pettitt, M. E.; Callow, M. E.; Callow, J. A. Settlement and Adhesion of Algal Cells to Hexa(Ethylene Glycol)-Containing Self-Assembled Monolayers with Systematically Changed Wetting Properties. *Biointerphases* **2007**, *2*, 143−150.
(8) Kang, S.; Asatekin, A.; Mayes, A. M.; Elimelech, M. Protein Antifouling Mechanisms of PAN UF Membranes Incorporating PAN-g-PEO Additive. *J. Membr. Sci.* **2007**, *296*, 42−50.
(9) Song, L.; Zhao, J.; Luan, S.; Ma, J.; Liu, J.; Xu, X.; Yin, J. Fabrication of a Detection Platform with Boronic-Acid-Containing Zwitterionic Polymer Brush. *ACS Appl. Mater. Interfaces* **2013**, *5*, 13207−13215.
(10) Chen, S.; Cao, Z.; Jiang, S. Ultra-Low Fouling Peptide Surfaces Derived from Natural Amino Acids. *Biomaterials* **2009**, *30*, 5892−5896.
(11) Blanco, C. D.; Ortner, A.; Dimitrov, R.; Navarro, A.; Mendoza, E.; Tzanov, T. Building an Antifouling Zwitterionic Coating on Urinary Catheters Using an Enzymatically Triggered Bottom-Up Approach. *ACS Appl. Mater. Interfaces* **2014**, *6*, 11385−11393.
(12) Gong, M.; Wang, Y.; Li, M.; Hu, B.; Gong, Y. Fabrication and Hemocompatibility of Cell Outer Membrane Mimetic Surfaces on Chitosan by Layer by Layer Assembly with Polyanion Bearing Phosphorylcholine Groups. *Colloids Surf., B* **2011**, *85*, 48−55.
(13) Ma, Q.; Zhang, H.; Zhao, J.; Gong, Y. Fabrication of Cell Outer Membrane Mimetic Polymer Brush on Polysulfone Surface via RAFT Technique. *Appl. Surf. Sci.* **2012**, *258*, 9711−9717.
(14) Gong, M.; Dang, Y.; Wang, Y.; Yang, S.; Winnik, F. M.; Gong, Y. Cell Membrane Mimetic Films Immobilized by Synergistic Grafting and Crosslinking. *Soft Matter* **2013**, *9*, 4501−4508.
(15) Thérien-Aubin, H.; Huang, X.; Hoek, E. M. V.; Ober, C. K. Antifouling Properties of Functionalized Polyaramide Membranes. *Polym. Prepr.* **2010**, *51*, 377−378.
(16) Thérien-Aubin, H.; Chen, L.; Ober, C. K. Fouling-Resistant Polymer Brush Coatings. *Polymer* **2011**, *52*, 5419−5425.
(17) Hlady, V.; Buijs, J.; Jennissen, H. P. Methods for Studying Protein Adsorption. *Methods Enzymol.* **1999**, *309*, 402−429.
(18) Lenk, T. J.; Horbett, T. A.; Ratner, B. D.; Chittur, K. K. Infrared Spectroscopic Studies of Time-Dependent Changes in Fibrinogen Adsorbed to Polyurethanes. *Langmuir* **1991**, *7*, 1755−1764.
(19) Liley, M.; Keller, T. A.; Duschl, C.; Vogel, H. Direct Observation of Self-Assembled Monolayers, Ion Complexation, and Protein Conformation at the Gold/Water Interface: An FTIR Spectroscopic Approach. *Langmuir* **1997**, *13*, 4190−4192.
(20) Chittur, K. K. FTIR/ATR for Protein Adsorption to Biomaterial Surfaces. *Biomaterials* **1998**, *19*, 357−369.
(21) Schartner, J.; Güldenhaupt, J.; Mei, B.; Rögner, M.; Muhler, M.; Gerwert, K.; Kötting, C. Universal Method for Protein Immobilization on Chemically Functionalized Germanium Investigated by ATR-FTIR Difference Spectroscopy. *J. Am. Chem. Soc.* **2013**, *135*, 4079−4087.
(22) Simón-Vázquez, R.; Lozano-Fernández, T.; Peleteiro-Olmedo, M.; González-Fernández, Á. Conformational Changes in Human Plasma Proteins Induced by Metaloxide Nanoparticles. *Colloids Surf., B* **2014**, *113*, 198−206.
(23) Roach, P.; Farrar, D.; Perry, C. C. Interpretation of Protein Adsorption: Surface-Induced Conformational Changes. *J. Am. Chem. Soc.* **2005**, *127*, 8168−8173.
(24) Sota, H.; Hasegawa, Y.; Iwakura, M. Detection of Conformational Changes in an Immobilized Protein Using Surface Plasmon Resonance. *Anal. Chem.* **1998**, *70*, 2019−2024.
(25) Feng, J.; Wang, W.; Li, J.; Fu, L.; Zhao, J.; Qiao, Y.; Sun, P.; Yuan, Z. Effects of Oligopeptide's Conformational Changes on Its Adsorption. *Colloids Surf., B* **2011**, *83*, 229−236.
(26) Lehnert, M.; Gorbahn, M.; Rosin, C.; Klein, M.; Köper, I.; Al-Nawas, B.; Knoll, W.; Veith, M. Adsorption and Conformation Behavior of Biotinylated Fibronectin on Streptavidin-Modified TiO_X Surfaces Studied by SPR and AFM. *Langmuir* **2011**, *27*, 7743−7751.
(27) Reviakine, I.; Johannsmann, D.; Richter, R. P. Hearing What You Cannot See and Visualizing What You Hear: Interpreting Quartz Crystal Microbalance Data from Solvated Interfaces. *Anal. Chem.* **2011**, *83*, 8838−8848.
(28) Delcroix, M. F.; Demoustier-Champagne, S.; Dupont-Gillain, C. C. Quartz Crystal Microbalance Study of Ionic Strength and pH-Dependent Polymer Conformation and Protein Adsorption/Desorption on PAA, PEO, and Mixed PEO/PAA Brushes. *Langmuir* **2014**, *30*, 268−277.
(29) Inoue, Y.; Ishihara, K. Reduction of Protein Adsorption on Well-Characterized Polymer BrushLayers with Varying Chemical Structures. *Colloids Surf., B* **2010**, *81*, 350−357.
(30) Höök, F.; Rodahl, M.; Brezinski, P.; Kasemo, B.; Brezinski, P. Structural Changes in Hemoglobin During Adsorption to Solid-Surfaces: Effects of pH, Ionic Strength, and Ligand Binding. *Proc. Natl. Acad. Sci. U.S.A.* **1998**, *95*, 12271−12276.
(31) Liu, G.; Zhang, G. Collapse and Swelling of Thermally Sensitive Poly(N-isopropylacrylamide) Brushes Monitored with a Quartz Crystal Microbalance. *J. Phys. Chem. B* **2005**, *109*, 743−747.
(32) Liu, G.; Zhang, G. Reentrant Behavior of Poly(N-isopropylacrylamide) Brushes in Water-Methanol Mixtures Investigated with a Quartz Crystal Microbalance. *Langmuir* **2005**, *21*, 2086−2090.
(33) Liu, G.; Yan, L.; Chen, X.; Zhang, G. Study of the Kinetics of Mushroom-to-Brush Transition of Charged Polymer Chains. *Polymer* **2006**, *47*, 3157−3163.
(34) Mrksich, M.; Sigal, G. B.; Whitesides, G. M. Surface Plasmon Resonance Permits in Situ Measurementof Protein Adsorption on Self-Assembled Monolayers of Alkanethiolates on Gold. *Langmuir* **1995**, *11*, 4383−4385.
(35) Jung, L. S.; Campbell, C. T.; Chinowsky, T. M.; Mar, M. N.; Yee, S. S. Quantitative Interpretation of the Response of Surface

DOI: 10.1021/acsami.5b01138
ACS Appl. Mater. Interfaces 2015, 7, 6422−6429

Plasmon Resonance Sensors to Adsorbed Films. *Langmuir* **1998**, *14*, 5636−5648.
(36) Craig, V. S. J.; Plunkett, M. Adsorbed Layer Structure of a Weak Polyelectrolyte Studied by Colloidal Probe Microscopy and QCM-D as a Function of pH and Ionic Strength. *J. Colloid Interface Sci.* **2003**, *262*, 126−129.
(37) Notley, S. M.; Biggs, S.; Craig, V. S. J.; Wågberg, L. Quantitative Interpretation of the Response of Surface Plasmon Resonance Sensors to Adsorbed Films. *Phys. Chem. Chem. Phys.* **2004**, *6*, 2379−2386.
(38) Zhu, M. Q.; Wang, L. Q.; Exarhos, G. J.; Li, A. D. Q. Thermosensitive Gold Nanoparticles. *J. Am. Chem. Soc.* **2004**, *126*, 2656−2657.
(39) Sauerbrey, G. Verwendung von Schwingquarzen zur Wägung-dünner Schichten und zur Mikrowägung. *Z. Phys.* **1959**, *155*, 206−222.
(40) Rodahl, M.; Höök, F.; Krozer, A.; Kasemo, B.; Breszinsky, P. Quartz-Crystal Microbalance Setup for Frequency and Q-FactorMeasurements in Gaseous and Liquid Environments. *Rev. Sci. Instrum.* **1995**, *66*, 3924−3930.
(41) Stenberg, E.; Persson, B.; Roos, H.; Urbaniczky, C. Quantitative Determination of Surface Concentration of Protein with Surface Plasmon Resonance Using Radiolabeled Proteins. *J. Colloid Interface Sci.* **1991**, *143*, 513−526.
(42) Liu, X.; Sun, K.; Wu, Z.; Lu, J.; Song, B.; Tong, W.; Shi, X.; Chen, H. Facile Synthesis of Thermally Stable Poly(N-vinylpyrrolidone)-Modified Gold Surfaces by Surface-Initiated Atom Transfer RadicalPolymerization. *Langmuir* **2012**, *28*, 9451−9459.
(43) Bhuchar, N.; Deng, Z.; Ishihara, K.; Narain, R. Detailed Study of the Reversible Addition−Fragmentation Chain Transfer Polymerization and Co-Polymerization of 2-Methacryloyloxyethyl Phosphorylcholine. *Polym. Chem.* **2011**, *2*, 632−639.
(44) The information of RAFT agents suited for various monomer types can be seen in CSIRO's RAFT agent monomer matching guide: http://www.csiro.au/en/Organisation-Structure/Divisions/CMSE/RAFT-technologies/What-is-RAFT.aspx.
(45) Ejaz, M.; Ohno, K.; Tsujii, Y.; Fukuda, T. Controlled Grafting of a Well-Defined Glycopolymer on a Solid Surface by Surface-Initiated Atom Transfer Radical Polymerization. *Macromolecules* **2000**, *33*, 2870−2874.
(46) Kitano, K.; Inoue, Y.; Matsuno, R.; Takai, M.; Ishihara, K. Nanoscale Evaluation of Lubricity on Well-Defined Polymer Brush Surfaces Using QCM-D and AFM. *Colloids Surf., B* **2009**, *74*, 350−357.
(47) Morse, A. J.; Edmondson, S.; Dupin, D.; Armes, S. P.; Zhang, Z.; Leggett, G. J.; Thompson, R. L.; Lewis, A. L. Biocompatible Polymer Brushes Grown from Model Quartz Fibres: Synthesis, Characterisation and in situ Determination of Frictional Coefficient. *Soft Matter* **2010**, *6*, 1571−1579.
(48) Yim, H.; Kent, M. S.; Satija, S.; Mendez, S.; Balamurugan, S. S.; Balamurugan, S.; Lopez, G. P. Evidence for Vertical Phase Separation in Densely Grafted, High-Molecular-Weight Poly(N-isopropylacrylamide) Brushes in Water. *Phys. Rev. E* **2005**, *72*, 051801.
(49) Wu, T.; Gong, P.; Szleifer, I.; Vlček, P.; Sÿubr, V.; Genzer, J. Behavior of Surface-Anchored Poly(acrylic acid) Brushes with Grafting Density Gradients on Solid Substrates: 1. Experiment. *Macromolecules* **2007**, *40*, 8756−8764.
(50) Salas, C.; Rojas, O. J.; Lucia, L. A.; Hubbe, M. A.; Genzer, J. On the Surface Interactions of Proteins with Lignin. *ACS Appl. Mater. Interfaces* **2013**, *5*, 199−206.
(51) Salas, C.; Genzer, J.; Lucia, L. A.; Hubbe, M. A.; Rojas, O. J. Water-Wettable Polypropylene Fibers by Facile Surface Treatment Based on Soy Proteins. *ACS Appl. Mater. Interfaces* **2013**, *5*, 6541−6548.
(52) Slavin, S.; Soeriyadi, A. H.; Voorhaar, L.; Whittaker, M. R.; Becer, C. R.; Boyer, C.; Davis, T. P.; Haddleton, D. M. Adsorption Behaviour of Sulfur Containing Polymers to Gold Surfaces Using QCM-D. *Soft Matter* **2012**, *8*, 118−128.
(53) Zareie, H. M.; Boyer, C.; Bulmus, V.; Nateghi, E.; Davis, T. P. Temperature-Responsive Self-Assembled Monolayers of Oligo(ethylene glycol): Control of Biomolecular Recognition. *ACS Nano* **2008**, *2*, 757−765.
(54) Squire, P. G.; Moser, P.; O'Konski, C. T. The Hydrodynamic Properties of Bovine Serum Albumin Monomer and Dimer. *Biochemistry* **1968**, *7*, 4261−4272.

DOI: 10.1021/acsami.5b01138
ACS Appl. Mater. Interfaces 2015, 7, 6422−6429